Chinese Chemical Letters 32 (2021) 2513–2518

Contents lists available at ScienceDirect

Chinese Chemical Letters

journal homepage: www.elsevier.com/locate/cclet

Communication

Compared catalytic properties of OMS-2-based nanocomposites for the degradation of organic pollutants

Wenxin Hou[a,1], Shuhui Wang[a,1], Xiuru Bi[b,1], Xu Meng[b,**], Peiqing Zhao[b], Xiang Liu[a,c,*]

[a] College of Materials and Chemical Engineering, Key Laboratory of Inorganic Nonmetallic Crystalline and Energy Conversion Materials, Analysis and Testing Center, China Three Gorges University, Yichang 443002, China
[b] State Key Laboratory for Oxo Synthesis and Selective Oxidation, Suzhou Research Institute of LICP, Lanzhou Institute of Chemical Physics (LICP), Chinese Academy of Sciences, Lanzhou 730000, China
[c] Engineering Research Center of Eco-Environment in Three Gorges Reservoir Region, Ministry of Education, China Three Gorges University, Yichang 443002, China

ARTICLE INFO

Article history:
Received 25 October 2020
Received in revised form 8 December 2020
Accepted 12 January 2021
Available online 27 January 2021

Keywords:
OMS-2
Phosphotungstic acid
Organic pollutants
Degradation
Tungsten

ABSTRACT

In this study, Mn catalysts have been designed based on manganese oxide octahedral molecular sieve (OMS-2) supports to optimize the catalytic activity in the degradation of organic pollutants. Herein, two different synthetic strategies: Pre-incorporation *vs.* wet-impregnation have been employed to synthesize [PW]-OMS-2 and [PW]/OMS-2. For [PW]-OMS-2, energy dispersive X-ray spectroscopy (EDX) confirmed that dispersed granular phosphotungstic acid attached and located at the surface of OMS-2, meanwhile some W atoms have been doped into frameworks of OMS-2. However, for [PW]/OMS-2, the W atoms cannot enter the OMS-2 frameworks. A correlation has been established between the different synthetic strategies and catalytic activities. The [PW]-OMS-2 is the most highly effective and stable over than [PW]/OMS-2 and OMS-2 itself for the organic pollutants removal. This may be caused not only by the synergetic effect of [PW] and OMS-2, but also by doping W into frameworks of OMS-2. Therefore, this work provides a new environmentally-friendly and heterogeneous PMS activator and it may be put into practice to degrade organic pollutants.

Over the last few decades, the wantonly emission of organic dyes, such as rhodamine B (RhB), reactive red 2 (RR2), acid orange 7 (AO7), and reactive blue 19 (RB19), by the textile industry in municipal wastewater effluents and natural aquatic systems have particularly become globally environmental and public health problems due to their complex structure, stability and non-biodegradation [1]. Most of organic dyes induce mutagenic, carcinogenic or teratogenic effects in the human body, even a low concentration [2]. It is highly necessary to explore environmentally friendly, low-cost and effective methodologies for the removal of organic dyes in wastewater [3]. There have been many studies reporting on the removal of synthetic dyes from wastewater, including *via* adsorption, flocculation, biological degradation, photo-Fenton, membrane separation, Fenton-like and electrochemical degradation [4]. Among them, peroxymonosulfate (HSO_5^-, PMS) based advanced oxidation processes (AOPs) have attracted increasing attention in the rapid degradation of organic dyes in aqueous media. Sulfate radical ($SO_4^{\bullet-}$), derived from the activation of PMS, has a higher redox potential (E^o = 2.5–3.1 V *vs.* 1.8–2.7 V), greater activity, a longer half-life ($t_{1/2}$ = 30–40 μs *vs.* 20 ns) and higher mineralization ability toward organic dyes, compared to hydroxyl radical ($^{\bullet}OH$) [5]. In fact, a variety of heterogeneous catalysts including Co–, Fe– Ag–, Cu–, and Ru-based materials have been developed for effectively activating PMS in the degradation of organic dyes [6].

Since Wang's group first reported the Co_3O_4/MnO_2 catalyst in PMS based-AOP for effectively degrading phenol in 2012 [7], increasing interests have been paid to the exploration of manganese oxide octahedron molecular sieve OMS-2, a composition of KMn_8O_{16} with a 0.46 nm × 0.46 nm tunnels, for activation of PMS on the removal of organic pollutants, due to its mixed valences of Mn^{2+}, Mn^{3+} and Mn^{4+}, low toxicity, highly porous structure, low cost and environmental friendliness [8]. In order to improve catalytic activity, OMS-2 has been usually doped with transition

* Corresponding author at: College of Materials and Chemical Engineering, Key Laboratory of Inorganic Nonmetallic Crystalline and Energy Conversion Materials, Analysis and Testing Center, China Three Gorges University, Yichang 443002, China.
** Corresponding author.
E-mail addresses: xumeng@licp.cas.cn (X. Meng), xiang.liu@ctgu.edu.cn (X. Liu).
[1] These authors contributed equally to this work.

https://doi.org/10.1016/j.cclet.2021.01.023

metal ions, including Co^{2+}, Fe^{3+}, Cr^{3+}, Ce^{3+}, Cu^{2+}, V^{5+} and Mo^{6+}, by reflux, ball milling, hydrothermal method and impregnation [9]. It is clear that metal dopants in the tunnel structure or framework of OMS-2 could increase more defects and simultaneously create more active sites [10]. Among these transition metal ions, tungsten ion has been found to be a very important promoter to improve the catalytic activity and stabilize the active phase. Because tungsten ion (W^{6+}: 0.60 Å) has mostly same ionic radius as Mn ion (Mn^{3+}: 0.645 Å, Mn^{4+}: 0.53 Å) in edge-shared MnO_6 octahedra [11–13]. In 2020, our group first reported [PW]-OMS-2 nanocomposites, comprised of phosphotungstic acid [PW] and OMS-2, as an efficient reusable heterogeneous catalyst for the remarkably enhanced catalytic oxidative dehydrogenation of N-heterocycles [14]. As a part of our current studies on the development in the synthesis and application of OMS-2-based nanocomposites [15], herein, we are employing two different synthetic strategies: Pre-incorporation *vs.* wet-impregnation to synthesize [PW]-OMS-2 and [PW]/OMS-2 for optimizing the catalytic activity in the degradation of organic pollutants, such as RhB, RR2, A07 and RB19, for the first time. Among them, [PW]-OMS-2 has been synthesized from potassium permanganate, manganese sulfate and sodium phosphotungstate *via* the pre-incorporation method, while [PW]/OMS-2 catalyst is obtained by wet-impregnation of OMS-2 in phosphotungstic acid solution, summarized in Figs. S1 and S2 (Supporting information). The [PW]-OMS-2 is found to be the most highly effective and stable over than [PW]/OMS-2 and OMS-2 itself for the degradation of organic pollutants, in contrast with our previous Cu catalysts, where Cu-OMS-2 (pre-incorporation) shows less catalytic activity for reduction and click reaction, and no catalytic activity for homocoupling in comparison with CuO_x/OMS-2 (wet-impregnation) [15b]. Moreover, as-synthesized [PW]-OMS-2 has been successfully recycled at least 5 times without any significant activity loss in the degradation of diverse organic pollutants *via* PMS activation.

Based on our previous work, [PW]-OMS-2 **I–V** had been synthesized from potassium permanganate, manganese sulfate and different amounts of sodium phosphotungstate (sodium phosphotungstate/$KMnO_4$ ratios of 1 mol%, 2 mol%, 3 mol%, 4 mol% and 5 mol%) through the pre-incorporation method (Fig. S1). We confirmed that $Na_3O_{40}PW_{12}{\cdot}xH_2O$ was transformed into $Na_2WO_4{\cdot}2H_2O$ and $H_3[P(W_3O_{10})_4]{\cdot}xH_2O$ in heated solution [14]. The transmission electron microscope (TEM) images show that the low doping of sodium phosphotungstate (1 mol% and 2 mol%) does not change the structure and morphology of OMS-2, [PW]-OMS-2 **I** and **II** mostly remained the typical and uniform nanorod morphology as the OMS-2 (Figs. 1a–c). When the doping amount over than 2 mol%, the nanorod-like structure (such as [PW]-OMS-2 **III, IV** and **V**) became shorter and thicker (Figs. 1d–f). These catalysts had also been fully characterized by Inductively Coupled Plasma-Atomic Emission Spectrometry (ICP-AES), Brunauer Emmett Teller (BET), X-ray diffraction (XRD), scanning electron microscope (SEM), Transmission Electron Microscope (TEM), X-ray Photoelectron Spectroscopy (XPS), H_2-temperature programmed reduction (H_2-TPR), raman spectra and electron paramagnetic resonance spectra (EPR). Due to the doping of sodium phosphotungstate, [PW]-OMS-2 had newly-generated mixed crystal phases, an enhanced surface area and labile lattice oxygen [14]. In this work, their compared catalytic efficiency in the degradation of RhB in the presence of PMS has been investigated in Fig. 2. The degradation reaction was conducted with 50 mg/L RhB and 0.25 g/L PMS in the presence of 0.25 g/L OMS-2 or [PW]-OMS-2 **I–V** at 25 °C, respectively. RhB has been degraded totally in 6 min by [PW]-OMS-2 **II** and 45 min by OMS-2, respectively. It is clear that [PW]-OMS-2 **II** shows the highest degradation efficiency over than OMS-2 and other ones, consisting with our previous case of aerobic oxidative dehydrogenation of N-heterocycles [14]. Herein, for confirming localization of [PW] in the OMS-2, high-angle annular dark field-scanning transmission electron microscopy (HAADF-STEM) and energy dispersive X-ray spectrometer (EDX) mappings of [PW]-OMS-2 **II** has been measured. In Figs. 3a-f, the elements of O, P, K, Mn and W have been observed, indicating that the phosphotungstic acid and OMS-2 coexist in the [PW]-OMS-2 **II**

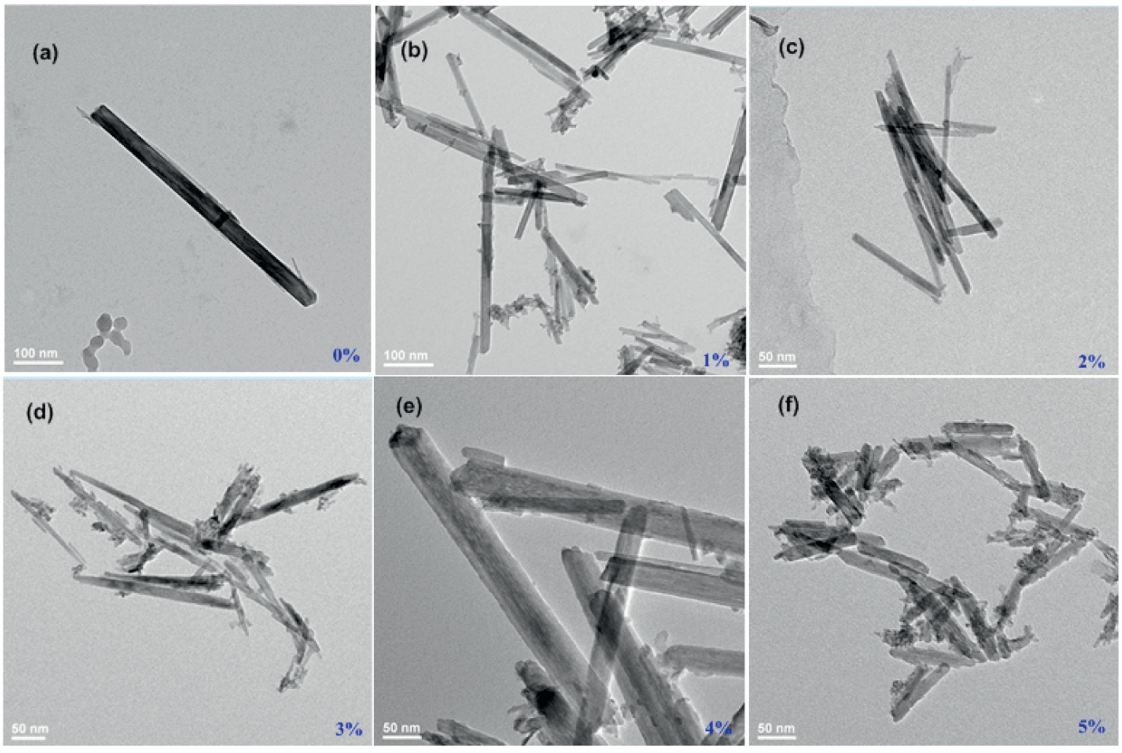

Fig. 1. TEM of (a) OMS-2, (b) [PW]-OMS-2 **I**, (c) [PW]-OMS-2 **II**, (d) [PW]-OMS-2 **III**, (e) [PW]-OMS-2 **IV** and (f) [PW]-OMS-2 **V.**

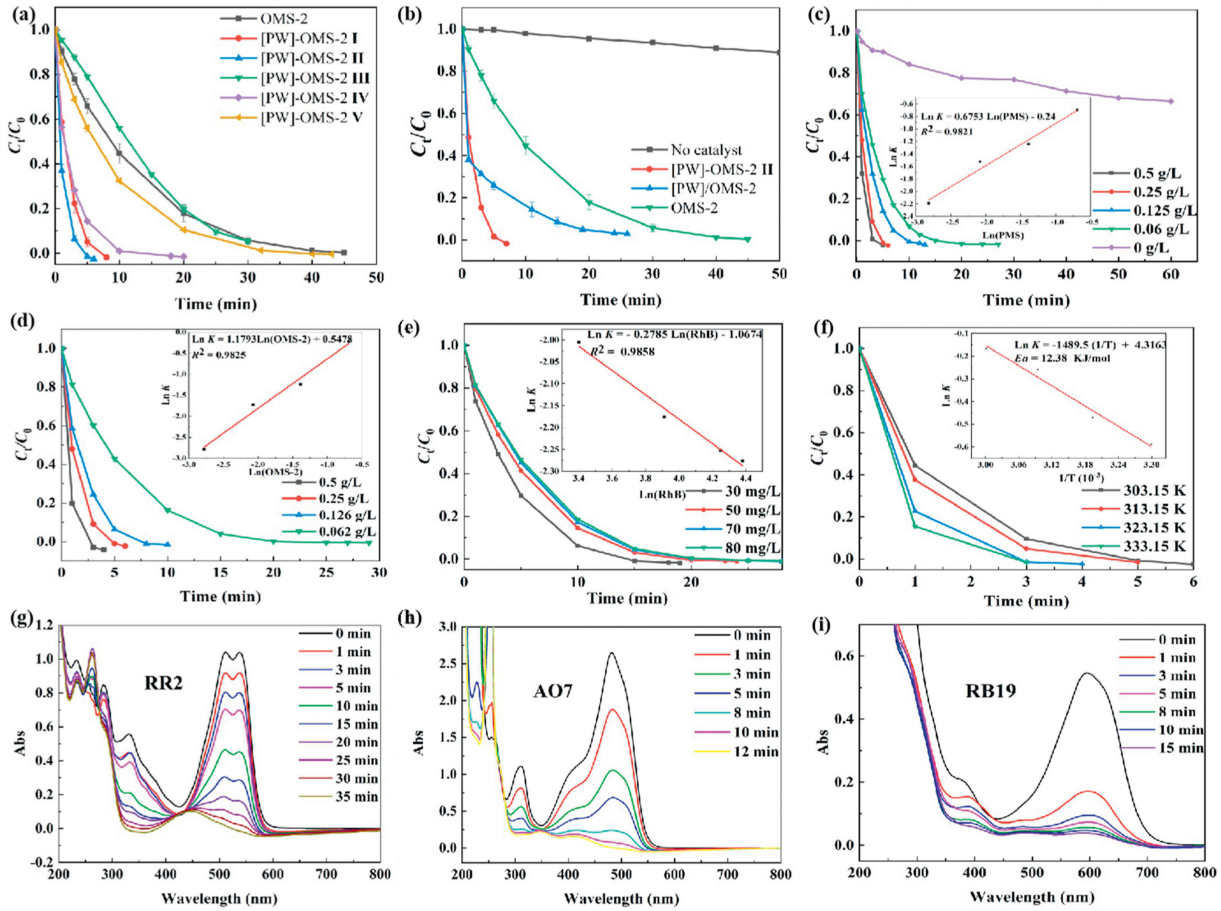

Fig. 2. (a) Degradation of RhB over OMS-2, [PW]-OMS-2 **I-V** catalysts. (b) Degradation of RhB over OMS-2, [PW]-OMS-2 **II** and **[**PW]/OMS-2; Influences of (c) the amount of PMS, (d) [PW]-OMS-2 **II** concentration, (e) initial RhB concentration and (f) reaction temperature on RhB degradation; [PW]-OMS-2 **II** catalyzed degradation of (g) RR2, (h) AO7 and (i) RB19 *via* PMS activation. Reaction conditions: (a-d, f, g-i): 0.25 g/L of cat, 50 mg/L of dyes, 0.25 g/L of PMS, 25 °C. (e) 0.126 g/L of [PW]-OMS-2 **II**, 0.126 g/L of PMS, 25 °C.

nanocomposite. The disappearance of Na element in the EDX map sum spectrum proves that it was washed away (Fig. S3 in Supporting information). Taking a cue from the STEM pictures of nanorods (Fig. 3g) and granular particles (Fig. 3h), respectively, the EDX spectrum of P and W confirmed that the grannular particle is $H_3[P(W_3O_{10})_4]\cdot xH_2O$, which is decomposed from $Na_3PO_4\cdot 12WO_3\cdot xH_2O$ (Fig. 3h and Fig. S4 in Supporting information), the unit cell size of phosphotungstic acid is 12 Å × 12 Å × 12 Å [16], so it cannot enter OMS-2 (4.6 Å × 4.6 Å). Whereas Fig. 3g and Fig. S5 (Supporting information) also verified only W, provided by $Na_2WO_4\cdot 2H_2O$, has been doped into frameworks of OMS-2. It is confirmed that dispersed granular phosphotungstic acid attached and located at the surface of OMS-2, meanwhile some W atoms were doped into frameworks of OMS-2. Furthermore, [PW]/OMS-2 catalyst was obtained by wet-impregnation of OMS-2 in phosphotungstic acid solution, with the same proportion of [PW]/$KMnO_4$ as for the former catalyst (Fig. S1). It is also conceivable that [PW] only attached and located at the surface of OMS-2, the W atoms cannot enter the OMS-2 frameworks. The SEM of [PW]/OMS-2 confirmed the predictable results (Fig. S6 in Supporting information). Obviously, the wet-impregnation method destroyed the uniform nanorod-like structure of OMS-2. Then the catalysts of [PW]-OMS-2 **II**, [PW]/OMS-2 and OMS-2 have been investigated for the degradation of RhB (Fig. 2b). [PW]-OMS-2 **II** exhibits highest efficiency for RhB degradation with a removal of 100% after 6 min in the presence of PMS at 25 °C. Whereas [PW]/OMS-2 and OMS-2 needs 26 min and 45 min, respectively. On the other hand, self-degradation of RhB is very weak (10%) under neutral conditions in the absence of catalyst (Fig. 2b). The order of catalytic activity follows: [PW]-OMS-2 **II** > [PW]/OMS-2 > OMS-2. The comparative experiment confirms that significant catalytic performance of [PW]-OMS-2 **II** is taken into account not only by the synergetic effect of [PW] and OMS-2, but also by doping W into frameworks of OMS-2. Compared to wet-impregnation, the pre-incorporation of [PW] and OMS-2 creates new mixed crystal phases, significantly enhanced surface area and more labile lattice oxygen. In addition, the comparision of PMS and H_2O_2 in the degradation of RhB shows that PMS is more efficient than that of H_2O_2 (Fig. S7 in Supporting information). Hence, [PW]-OMS-2 **II** has been chosen as the optimal catalyst for further degradation study *via* PMS activation.

The influences of several parameters including the concentrations of PMS, catalyst and initial RhB, and reaction temperature on RhB degradation are investigated in Figs. 2c–f. Fig. S8 (Supporting information) exhibits that the adsorption of RhB on the surface of [PW]-OMS-2 **II** is very weak (20%) over 60 min. These results suggest that the adsorption capacity of [PW]-OMS-2 **II** is negligible. An increase in PMS concentration from 0.062 g/L to 0.5 g/L has a distinct positive effect on the degradation of RhB (Fig. 2c). The slope of the logarithmic plot of RhB degradation *versus* concentration of PMS is 0.67, suggesting that the RhB degradation is the first order in PMS concentration. In similar, the slope of the logarithmic plot of RhB degradation *versus* catalyst concentration also exhibits that the reaction is first order in

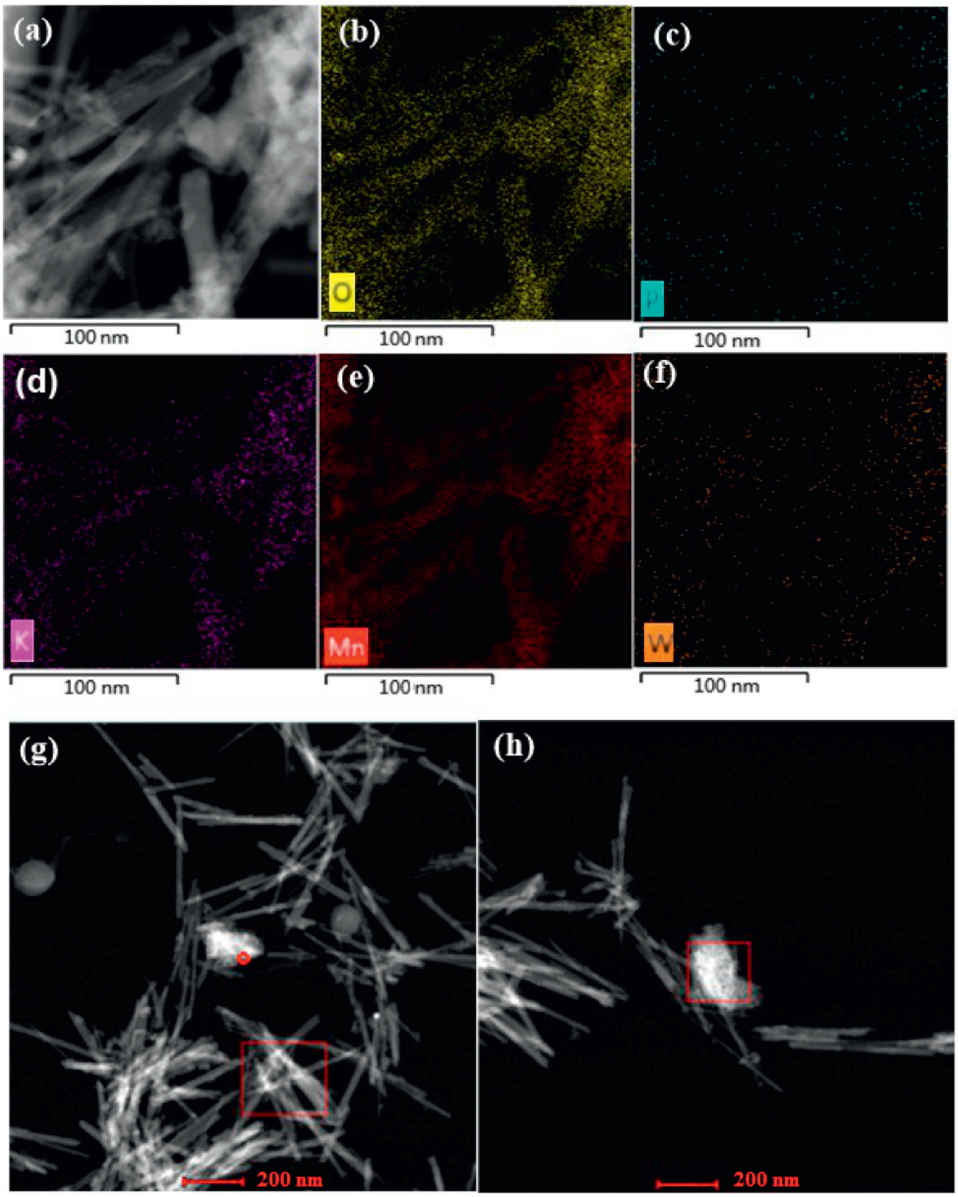

Fig. 3. (a) HAADF-STEM image, (b) O, (c) P, (d) K, (e) Mn and (f) W EDX compositional mapping of [PW]-OMS-2 **II**. HAADF-STEM-images of selected area of nanorod (g) and granualr particles (h).

catalyst concentration (Fig. 2d). The influences of initial RhB concentration from 30 mg/L to 80 mg/L on the RhB degradation was recorded in the Fig. 2e. The degradation efficiency of RhB were negatively correlated with initial RhB concentration. It is also the first order in the initial RhB concentration. Moreover, increasing reaction temperature is beneficial to enhance the ability of [PW]-OMS-2 **II** for activating PMS to generate reactive species (Fig. 2f). Based on the Arrhenius equation, the activation energy is calculated to be 12.38 kJ/mol, which is lower than that of OMS-2 (16.80 kJ/mol), indicating again that [PW]-doped OMS-2 is more superior on RhB degradation. In addition, the effect of pH on RhB degradation catalyzed by [PW]-OMS-2 **II** shows that pH appears more favorable at acidic pH (Fig. S9 in Supporting information).

To further explore the potential application of [PW]-OMS-2 **II** catalyst, different organic dyes such as the the azo RR2 (Fig. 2g), AO7 (Fig. 2h) and the disodium salt RB19 (Fig. 2i) have been investigated under standard conditions. These results show that RR2, AO7 and RB19 has been degraded completely in 35 min, 12 min and 15 min, respectively. According to the relevant published literature [5], the involved radicals in the current system are $SO_4^{\bullet-}$, $^{\bullet}OH$, $^1O_2$ and $O_2^{\bullet-}$. To understand the contribution of the individual radicals, free radical quenching experiments were undertaken in the Fig. 4a. EtOH, *t*-BuOH (TBA), NaN_3 and benzoquinone (BQ) were employed as effective scavengers $SO_4^{\bullet-}$, $^{\bullet}OH$, $O_2^{\bullet-}$ and $^1O_2$ in the RhB degradation, respectively. The result shown that $^1O_2$ is the main active species in the RhB degradation process [17,18]. To further confirm the possible reactive oxygen species generated in the standard RhB degradation process, a series of EPR experiments using 5,5-dimethyl-1-pyrrolidine *N*-oxide (DMPO) and 2,2,6,6-tetramethyl-4-piperidone (TEMP) as the spin-trapping agents have been performed. In the Fig. 4b, the signals of DMPO-$^{\bullet}OH$, DMPO-$SO_4^{\bullet-}$ and DMPO-$O_2^{\bullet-}$ characterized by four peaks are observed. Furthermore, a high-intensity triple signal peak of TEMP-$^1O_2$ is observed on EPR spectra, confirming the emergence of $^1O_2$ in the reaction system. EPR spectra shown that the existence of $SO_4^{\bullet-}$, $^{\bullet}OH$, $^1O_2$ and $O_2^{\bullet-}$, in contrast with OMS-2/PMS degradation process for which only $SO_4^{\bullet-}$ and $^{\bullet}OH$ are generated [7,15]. In this study, the $^1O_2$ played the most dominant

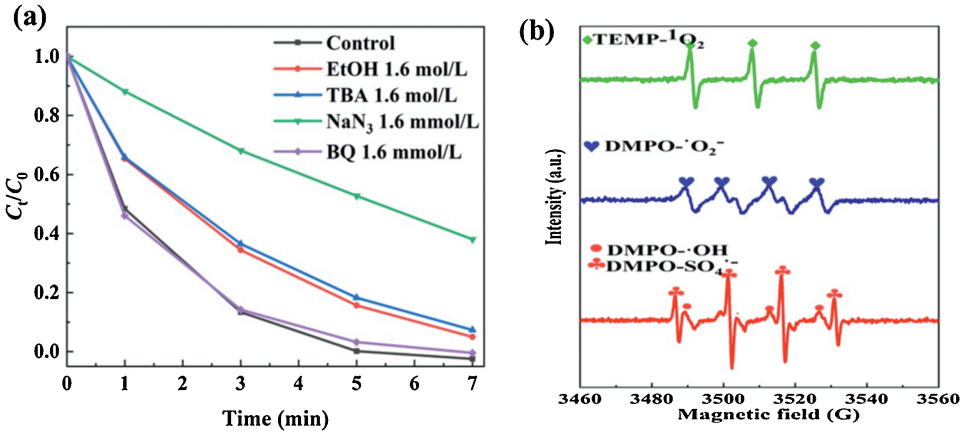

Fig. 4. (a) Inhibiter effect of EtOH, TBA, NaN_3 and BQ for degradation of RhB over [PW]-OMS-2 **II** with PMS. Reaction conditions: 0.25 g/L of [PW]-OMS-2 **II**, 0.25 g/L of PMS, 50 mg/L of RhB, 25 °C. (b) EPR spectrum for different system with DMPO or TEMP. Reaction conditions: 0.25 g/L of [PW]-OMS-2 **II**, 0.25 g/L of PMS, 5 mmol/L of DMPO or TEMP, 25 °C.

role in the degradation, it may be caused not only by the synergetic effect of [PW] and OMS-2, but also by doping W into frameworks of OMS-2.

To evaluate the stability and reusability of [PW]-OMS-2 **II** in heterogeneous reaction system, the degradation of RhB has been successfully recycled 5 times with the used catalyst (Fig. S10 in Supporting information). The degradation efficiency of RhB for the 1st round to the 5th round decreased very slightly. Besides, the 5th used catalyst has been characterized by TEM and XRD. Fig. S11 (Supporting information) exhibits that the morphology of 5th used [PW]-OMS-2 **II** remains typical and uniform nanorod morphology as the fresh catalyst (the JCPDS No. 80-0382). Taken together, this demonstrates that [PW]-OMS-2 **II** is very stable.

In summary, two different synthetic strategies: pre-incorporation *vs.* wet-impregnation have been employed to synthesize [PW]-OMS-2 and [PW]/OMS-2 for the efficient degradation of organic pollutants (such as rhodamine B, reactive red 2, acid orange 7, and reactive blue 19) for the first time. The [PW]-OMS-2 **II** catalyst had been synthesized from potassium permanganate, manganese sulfate and sodium phosphotungstate through the pre-incorporation method, while [PW]/OMS-2 catalyst was obtained by wet-impregnation of OMS-2 in phosphotungstic acid solution. The [PW]-OMS-2 **II** is found to be the most highly effective and stable over than [PW]/OMS-2 and OMS-2 itself for the degradation of organic pollutants, in contrast with our previous Cu catalysts. Based on the Arrhenius equation, the activation energy of [PW]-OMS-2 **II** is calculated to be 12.38 kJ/mol, which is lower than that of OMS-2 (16.80 kJ/mol). The free radical quenching experiments and EPR spectra confirm that the existence of $SO_4^{\bullet-}$, $^{\bullet}OH$, $^1O_2$ and $O_2^{\bullet-}$ in the [PW]-OMS-2 **II**/PMS system, in contrast with OMS-2/PMS degradation process for which only $SO_4^{\bullet-}$ and $^{\bullet}OH$ are generated [7,15]. In this study, the $^1O_2$ played the most dominant role in the degradation, it may be caused not only by the synergetic effect of [PW] and OMS-2, but also by doping W into frameworks of OMS-2. In addition, as-synthesized [PW]-OMS-2 **II** has been successfully recycled at least 5 times without any significant activity loss in the degradation of diverse organic pollutants *via* PMS activation. This work provides an environmentally friendly and heterogeneous catalyst for the wastewater remediation.

Declaration of competing interest

The authors declare that they have no known competing financial interests or personal relationships that could have appeared to influence the work reported in this paper.

Acknowledgments

This work was supported by the National Natural Science Foundation of China (Nos. 21805166, 21403256 and 21573261), the 111 Project (No. D20015) and the Engineering Research Center of Eco-environment in Three Gorges Reservoir Region, Ministry of Education, China Three Gorges University (No. KF2019-05), the Outstanding Young and Middle-Aged Science and Technology Innovation Teams, Ministry of Education, Hubei province, China (No. T2020004), the Youth Innovation Promotion Association CAS (No. 2018456) and LICP Cooperation Foundation for Young Scholars (No. HZJJ20-10).

Appendix A. Supplementary data

Supplementary material related to this article can be found, in the online version, at doi:https://doi.org/10.1016/j.cclet.2021.01.023.

References

[1] (a) F. Lu, D. Astruc, Coord. Chem. Rev. 356 (2018) 147–164;
(b) F. Lu, D. Astruc, Coord. Chem. Rev. 408 (2020) 213180;
(c) E. Forgacs, T. Cserháti, G. Oros, Environ. Int. 30 (2004) 953–971;
(d) X. Sun, D. Xu, P. Dai, et al., Chem. Eng. J. 402 (2020) 125881;
(e) P. Duan, Y. Qi, S. Feng, et al., Appl. Catal. B: Environ. 267 (2020) 118717;
(f) E. Saputra, S. Muhammad, H. Sun, et al., Appl. Catal. B: Environ. 142-143 (2013) 729–735;
(g) S. Sun, H. Ding, L. Mei, Chen, et al., Chem. Lett. 31 (2020) 2287–2294;
(h) D. Yuan, M. Sun, S. Tang, et al., Chin. Chem. Lett. 31 (2020) 547–550;
(i) X. Lei, M. You, F. Pan, et al., Chem. Lett. 30 (2019) 2216–2220;
(j) J. Peng, Y. He, C. Zhou, S. Su, B. Lai, Chin. Chem. Lett. 32 (2021) 1626–1636;
(k) X. Yan, D. Yue, C. Guo, et al., Chin. Chem. Lett. 31 (2020) 1535–1539;
(l) J. Li, Y. Li, Z. Xiong, G. Yao, B. Lai, Chin. Chem. Lett. 30 (2019) 2139–2146;
(m) G. Elmaci, A.S. Ertürk, M. Sevim, Ö. Metin, Int. J. Hydrogen Energy 44 (2019) 17995.
[2] (a) M. Solís, A. Solís, H.I. Pérez, N. Manjarrez, M. Flores, Process Biochem. 47 (2012) 1723–1748;
(b) Z.H. Huang, Z.Y. Jia, Y.Y. Zhao, et al., Chem. Eng. J. 400 (2020) 125863;
(c) J. Lei, B. Chen, L. Zhou, et al., Chem. Eng. J. 400 (2020) 125902;
(d) B. Wu, S. Deng, H. Wang, G. Gu, Y. Wang, Chem. Eng. J. 401 (2020) 126105;
(e) H. Sun, F. Guo, J. Pan, et al., Chem. Eng. J. 406 (2020) 126844;
(f) A. Wang, Z. Zheng, H. Wang, et al., Appl. Catal. B: Environ. 277 (2020) 119171.
[3] (a) L. Pan, W. Shi, T. Sen, L. Wang, J. Zhang, Appl. Catal. B: Environ. 280 (2021) 119414;
(b) J. Wang, B. Xiong, L. Miao, et al., Appl. Catal. B: Environ. 280 (2021) 119422;
(c) Y. Gao, Q. Zhao, Y. Li, et al., Chem. Eng. J. 405 (2021) 126719;
(d) Y. Yu, Y. Ji, J. Lu, X. Yin, Q. Zhou, Chem. Eng. J. 406 (2021) 126759;
(e) R. Deng, Q. He, D. Yang, et al., Chem. Eng. J. 406 (2021) 126884;
(f) S. Xin, G. Liu, X. Ma, et al., Appl. Catal. B: Environ. 280 (2021) 119386;
(g) X. He, B. Sun, M. He, et al., Appl. Catal. B: Environ. 277 (2020) 119219;
(h) J.C.E. Yang, Y. Lin, H.H. Peng, et al., Appl. Catal. B: Environ. 268 (2020) 118549;

(i) J. Yang, D. Zeng, Q. Zhang, et al., Appl. Catal. B: Environ. 279 (2020) 119363;
(j) Z. Wang, H. Jia, T. Zheng, et al., Appl. Catal. B: Environ. 272 (2020) 119030;
(k) S. Shu, P. Wang, W. Zhang, et al., Chin. Chem. Lett. 31 (2020) 2762–2768;
(l) Y. Peng, M. Cui, Z. Zhang, et al., ACS Catal. 9 (2019) 10803–10811;
(m) G. Jiang, X. Li, Y. Shen, et al., J. Catal. 391 (2020) 414–423.
[4] (a) A. Roy, S. Chakraborty, S.P. Kundu, B. Adhikari, S.B. Majumder, Ind. Eng. Chem. Res. 51 (2012) 12095–12106;
(b) Y. Jia, L. Ding, P. Ren, et al., J. Chem. Eng. Data 65 (2020) 725–736;
(c) C.Y. Teh, P.M. Budiman, K.P.Y. Shak, T.Y. Wu, Ind. Eng. Chem. Res. 55 (2016) 4363–4389;
(d) J. Liu, J. Xiong, C. Tian, et al., Chem. Eng. J. 338 (2018) 719–725;
(e) L.I. Doumic, P.A. Soares, M.A. Ayude, et al., Chem. Eng. J. 277 (2015) 86–96;
(f) R. Mei, Q. Wei, C. Zhu, et al., Appl. Catal. B: Environ. 245 (2019) 420–427;
(g) A.A. Oladipo, A.O. Ifebajo, M. Gazi, Appl. Catal. B: Environ. 243 (2019) 243–252.
[5] (a) X. Liu, Y. Huang, P. Zhao, X. Meng, D. Astruc, ChemCatChem 12 (2020) 175–180;
(b) J. Huang, H. Zhang, Environ. Int. 133 (2019) 105141.
[6] H. Liang, H. Sun, A. Patel, et al., Appl. Catal. B: Environ. 127 (2012) 330–335.
[7] S. Luo, L. Duan, B. Sun, et al., Appl. Catal. B: Environ. 164 (2015) 92–99.
[8] (a) I.B. Alcover, S. Daviero-Minaud, R. David, et al., Inorg. Chem. 54 (2015) 8733–8743;
(b) M. Li, J. Zhang, J. Han, et al., Inorg. Chem. 56 (2017) 241–251;
(c) M. Zhou, L. Cai, M. Bajdich, et al., ACS Catal. 5 (2015) 4485–4491;
(d) C. Calvert, R. Joesten, K. Ngala, et al., Chem. Mater. 20 (2008) 6382–6388.
[9] (a) X.F. Shen, Y.S. Ding, J. Liu, et al., J. Am. Chem. Soc. 127 (2005) 6166–6167;
(b) S.L. Suib, J. Mater. Struct. Chem. 18 (2008) 1623–1631;
(c) M. Sun, L. Yu, F. Ye, et al., Chem. Eng. J. 220 (2013) 320–327;
(d) X. Xiao, S.P. Sun, M. McBride, A. Lemley, Environ. Sci. Pollut. Res. 20 (2013) 10–21;
(e) X.S. Liu, Z.N. Jin, J.Q. Lu, X.X. Wang, M.F. Luo, Chem. Eng. J. 162 (2010) 151–157;
(f) C.K. Kingondu, N. Opembe, C.H. Chen, et al., Adv. Funct. Mater. 21 (2011) 312–323;
(g) T. Uematsu, Y. Miyamoto, Y. Ogasawara, et al., Catal. Sci. Technol. 6 (2016) 222–233;
(h) L. Zhang, J. Tu, L. Lyu, C. Hu, Appl. Catal. B: Environ. 181 (2016) 561–569.
[10] (a) D.W. Kwon, K.B. Nam, S.C. Hong, Appl. Catal. A Gen. 497 (2015) 160–166;
(b) Z. Liu, H. Su, B. Chen, J. Li, S.I. Woo, Chem. Eng. J. 299 (2016) 255–262.
[11] J. Ma, J. Wang, Y. Dang, Chem. Eng. J. 388 (2020) 124387.
[12] F. Liu, R. Cao, S. Rong, P. Zhang, Mater Desig. 149 (2018) 165–172.
[13] Y. Yang, J. Jia, Y. Liu, P. Zhang, Appl. Catal. A: Gen. 562 (2018) 132–141.
[14] X. Bi, T. Tang, X. Meng, et al., Catal. Sci. Technol. 10 (2020) 360–371.
[15] (a) Y. Huang, Y. Wang, X. Meng, X. Liu, Inorg. Chem. Commun. 112 (2020) 107757;
(b) Y. Huang, K. Zheng, X. Liu, X. Meng, D. Astruc, Inorg. Chem. Front. 7 (2020) 939–945;
(c) Y. Huang, J. Yan, N. Zhang, et al., Catal. Lett. 150 (2020) 2021–2026;
(d) Y. Huang, Y. Wu, Y. Wang, X. Meng, X. Liu, ChemistrySelect 5 (2020) 3272–3277;
(e) W. Hou, Y. Huang, X. Liu, Catal. Lett. 150 (2020) 3017–3022;
(f) S. Wang, Y. Huang, X. Meng, X. Liu, Inorg. Chem. Commun. 112 (2020) 107969;
(h) L. Tao, X. Bi, L. Zhang, et al., Appl. Catal. A: Gen. 605 (2020) 117813.
[16] J.F. Keggin, Proc. R. Soc. Lond. A 144 (1934) 75–100.
[17] (a) S. Zhu, X. Li, J. Kang, X. Duan, S. Wang, Environ. Sci. Technol. 53 (2019) 307–315;
(b) H. Kim, W. Kim, Y. Mackeyev, et al., Environ. Sci. Technol. 46 (2012) 9606–9613.
[18] L. Kong, G. Fang, X. Xia, et al., Chem. Eng. J. 403 (2021) 126445.